

UC Davis

UC Davis Previously Published Works

Title

Substitutions in the presumed sensing domain of the *Bacillus subtilis* stressosome affect its basal output but not response to environmental signals.

Permalink

<https://escholarship.org/uc/item/0sj7b7bs>

Journal

Journal of bacteriology, 193(14)

ISSN

0021-9193

Authors

Gaidenko, Tatiana A
Bie, Xiaomei
Baldwin, Enoch P
et al.

Publication Date

2011-07-01

DOI

10.1128/jb.00060-11

Peer reviewed

Substitutions in the Presumed Sensing Domain of the *Bacillus subtilis* Stressosome Affect Its Basal Output but Not Response to Environmental Signals[∇]

Tatiana A. Gaidenko,¹ Xiaomei Bie,^{1†} Enoch P. Baldwin,² and Chester W. Price^{1*}

Departments of Microbiology¹ and Molecular & Cellular Biology,² One Shields Avenue,
University of California, Davis, California 95616

Received 12 January 2011/Accepted 15 April 2011

The stressosome is a multiprotein, 1.8-MDa icosahedral complex that transmits diverse environmental signals to activate the general stress response of *Bacillus subtilis*. The way in which it senses these cues and the pathway of signal propagation within the stressosome itself are poorly understood. The stressosome core consists of four members of the RsbR coantagonist family together with the RsbS antagonist; its cryo-electron microscopy (cryoEM) image suggests that the N-terminal domains of the RsbR proteins form homodimers positioned to act as sensors on the stressosome surface. Here we probe the role of the N-terminal domain of the prototype coantagonist RsbRA by making structure-based amino acid substitutions in potential interaction surfaces. To unmask the phenotypes caused by single-copy *rsbRA* mutations, we constructed strains lacking the other three members of the RsbR coantagonist family and assayed system output using a reporter fusion. Effects of five individual alanine substitutions in the prominent dimer groove did not match predictions from an earlier *in vitro* assay, indicating that the *in vivo* assay was necessary to assess their influence on signaling. Additional substitutions expected to negatively affect domain dimerization had substantial impact, whereas those that sampled other prominent surface features had no consequence. Notably, even mutations resulting in significantly altered phenotypes raised the basal level of system output only in unstressed cells and had little effect on the magnitude of subsequent stress signaling. Our results provide evidence that the N-terminal domain of the RsbRA coantagonist affects stressosome function but offer no direct support for the hypothesis that it is a signal sensor.

In *Bacillus subtilis* and its close relatives, the stressosome is a large cytoplasmic complex that converts diverse environmental signals, such as acid, ethanol, heat, or salt stress, to an output that activates the general stress factor σ^B (reviewed in references 12, 20, and 30). Key stressosome components are encoded by clustered genes in a variety of bacteria, including many that lack the σ^B transcription factor; these clusters are found in contexts suggesting involvement in a range of signaling pathways (29). The stressosome therefore represents a sensory machine whose output can be adapted to different tasks. However, there is limited understanding of the internal operation of the stressosome, even in the *B. subtilis* model.

Genetic and biochemical studies have shown that the *B. subtilis* stressosome comprises at least three protein species: the RsbT serine/threonine kinase, the RsbS antagonist, and one or more members of the RsbR coantagonist family (1, 9, 13, 24, 32). *In vivo* each stressosome appears to contain a mixture of the four partially redundant RsbR coantagonists, RsbRA, RsbRB, RsbRC, and RsbRD, and *in vitro* these coantagonists can dynamically exchange into the complex (13, 24). Cryo-electron microscopy (cryoEM) images of a minimal stressosome formed *in vitro* from purified RsbRA, RsbS, and RsbT

are consistent with a structure in which the STAS (sulfate transporter anti-anti- σ) domains of 20 RsbRA dimers and 20 RsbS monomers form an essentially icosahedral core that can bind 20 RsbT monomers, suggesting a mass of 1.8 MDa (26). According to the current model of the signaling network, RsbT is bound to RsbS in unstressed cells and is released when stress is sensed (Fig. 1). Free RsbT then binds and activates the RsbU environmental phosphatase, inducing the stress response via a signaling cascade that ultimately frees σ^B from its cognate anti- σ factor (20, 30).

The stressosome is thought to regulate the kinase activity of RsbT during the response, and RsbT phosphorylates the STAS domains of the RsbS and RsbR proteins on conserved serine and threonine residues, contributing to RsbT release (10, 16, 18, 35). Alteration of the conserved serine in RsbS (S59A) significantly weakens activation of the response, suggesting that S59 phosphorylation is important but not essential for signaling in otherwise wild-type cells (23). Similar alterations to conserved threonines in RsbRA, the prototype of the RsbR family, support the inference that phosphorylation of T171 is a prerequisite for signaling but does not by itself trigger the response; in contrast, the additional phosphorylation of T205 appears to attenuate the response in the face of extreme environmental stress (16, 24).

How might the stressosome sense input signals? In contrast to the RsbS antagonist, whose structure consists of a single STAS domain, the RsbR coantagonists each have two domains: a C-terminal STAS domain and an N-terminal, non-heme globin domain (26, 28). The isolated N-terminal domain

* Corresponding author. Mailing address: Department of Microbiology, One Shields Avenue, University of California, Davis, CA 95616. Phone: (530) 752-1596. Fax: (530) 752-9014. E-mail: cwprice@ucdavis.edu.

† Present address: Department of Bioengineering, Nanjing Agricultural University, Nanjing 210095, People's Republic of China.

[∇] Published ahead of print on 20 May 2011.

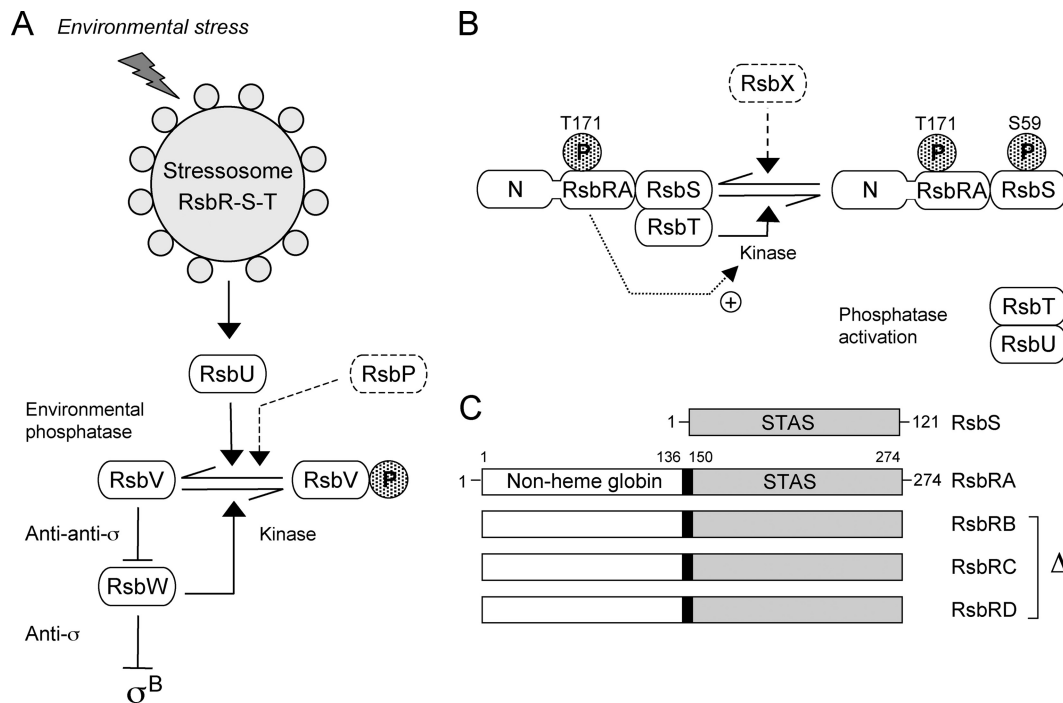


FIG. 1. σ^B regulatory network. (A) Model of signaling pathways that regulate σ^B (20, 30). Environmental and energy pathways converge on RsbV anti-anti- σ and RsbW anti- σ , which directly regulate σ^B . The multiprotein stressosome controls activation of the RsbU environmental phosphatase in response to diverse signals; the RsbP energy phosphatase is represented in dotted outline. Activated RsbU removes the phosphate (stippled P) from RsbV-P, the form found in unstressed cells, converting it to RsbV (horizontal arrows). RsbV binds RsbW, promoting σ^B release from the anti- σ . Arrowheads indicate activation of protein targets or enzymatic reactions; T-headed lines indicate inhibition. (B) Model of stressosome control of RsbU phosphatase activity. The stressosome comprises the partially redundant RsbRA, -B, -C, and -D coantagonists (represented here as RsbRA, with its N-terminal nonheme globin domain labeled N) and the RsbS antagonist, which together bind the RsbT kinase. In unstressed cells, RsbT phosphorylates RsbRA on T171. During the stress response, RsbRA-T171-P is an activator (+ arrow) of the RsbT kinase, which phosphorylates its RsbS antagonist on S59; RsbT is released to bind and activate RsbU. The RsbX feedback phosphatase is represented in dotted outline; it dephosphorylates RsbS-P, damping continued signaling. (C) The RsbS antagonist comprises a single STAS domain (residues 1 to 121), whereas the RsbRA coantagonist comprises a nonheme globin domain (residues 1 to 136) and a STAS domain (residues 150 to 274) joined by a 13-residue α -helical linker (black rectangle). The RsbRB, -C, and -D paralogs are structurally similar to RsbRA; these three paralogs have been removed from the key strains used in this study.

of RsbRA dimerizes *in vitro*, and cryoEM images of wild-type and mutant stressosomes indicate that these N-terminal dimers form turret-like projections that extend outward from the icosahedral core. Marles-Wright et al. (26) therefore proposed that the N-terminal, nonheme globin domains of the RsbR proteins are positioned to act as sensors, passing the signal to their C-terminal STAS domains via a 13-residue helical connector. Presumably, conformational changes in the STAS domains of the RsbR proteins are communicated to the STAS domains of neighboring RsbS proteins, promoting RsbT release.

Although this proposal is attractive, there is presently limited experimental evidence to support it. In one study, Murray et al. (28) found that some substitutions within the N-terminal domain of RsbRA prevented RsbT binding to the stressosome *in vitro*, whereas other substitutions did not. However, none of these was assayed to determine the phenotype *in vivo*. In another study, Reeves and Haldenwang (31) identified one substitution in the N-terminal region of RsbRA that elicited high σ^B activity in unstressed cells, but this change appeared to have only minor influence on environmental signaling.

Here we probe the *in vivo* function of the N-terminal domain of RsbRA by assaying the same substitutions that emerged

from these prior studies, using a genetic background in which their effects would be clearly apparent. We included in our study additional alterations to the domain surface that might be expected to affect dimerization or interaction with other signaling components. Although some of the tested substitutions had a striking influence on function in unstressed cells, none significantly affected environmental signaling.

MATERIALS AND METHODS

Bacterial strains and genetic methods. *B. subtilis* strains are shown in Table 1; plasmids used for strain construction are shown in Table 2. We used standard recombinant DNA methods (33) and performed natural transformation of *B. subtilis* strains as described by Dubnau and Davidoff-Abelson (14). Deletion and point mutations were introduced into *B. subtilis* strains using the I-SceI-mediated allele exchange method of Janes and Stibitz (22). For these exchanges, pSS4332 was the source of I-SceI restriction enzyme, and we constructed the companion integrative plasmid pTG5916 by adding an I-SceI site to pUS19. pTG5916 served as the basis for all plasmid constructions containing mutated *rsb* genes, as follows. (i) In-frame deletions in *rsbRA*, *rsbRB*, and *rsbRD* were created with four-primer PCR (21), and the appropriate fragments were cloned into pTG5916. (ii) Site-directed mutagenesis used a QuikChange Lightning kit (Stratagene, La Jolla, CA) to alter the pTG5923 template, which carried an *rsbRA* fragment cloned into pTG5916. (iii) The RsbS S59A substitution was introduced using pTG6009, which carried a mutant *rsbS* amplified by PCR from strain PB470 and cloned into pTG5916. In these strains, σ^B activity was measured indirectly

TABLE 1. *Bacillus subtilis* strains

Strain	Genotype	Reference/construction ^a
PB2	<i>trpC2</i>	168 Marburg strain
PB198	<i>amyE::ctc-lacZ trpC2</i>	8
PB470	<i>rsbS</i> S59A <i>amyE::ctc-lacZ trpC2</i>	23
PB1030	<i>rsbRBΔ2 trpC2</i>	pTG5925 → PB2 ^b
PB1070	<i>rsbRBΔ2 rsbRDΔ2 trpC2</i>	pTG5943 → PB1030 ^b
PB1071	<i>rsbRBΔ2 rsbRDΔ2 amyE::ctc-lacZ trpC2</i>	pDH32-ctc ^c → PB1070
PB1078	<i>rsbRBΔ2 rsbRCΔ1::ery rsbRDΔ2 amyE::ctc-lacZ trpC2</i>	pSA82 ^c → PB1071
PB1079	<i>rsbRA</i> E60A <i>rsbRBΔ2 rsbRCΔ1::ery rsbRDΔ2 amyE::ctc-lacZ trpC2</i>	pTG5924 → PB1078 ^b
PB1080	<i>rsbRA</i> K82A <i>rsbRBΔ2 rsbRCΔ1::ery rsbRDΔ2 amyE::ctc-lacZ trpC2</i>	pTG5926 → PB1078 ^b
PB1081	<i>rsbRA</i> E126A <i>rsbRBΔ2 rsbRCΔ1::ery rsbRDΔ2 amyE::ctc-lacZ trpC2</i>	pTG5927 → PB1078 ^b
PB1092	<i>rsbRA</i> T86A <i>rsbRBΔ2 rsbRCΔ1::ery rsbRDΔ2 amyE::ctc-lacZ trpC2</i>	pTG5944 → PB1078 ^b
PB1093	<i>rsbRA</i> N129A <i>rsbRBΔ2 rsbRCΔ1::ery rsbRDΔ2 amyE::ctc-lacZ trpC2</i>	pTG5945 → PB1078 ^b
PB1102	<i>rsbRA</i> Y35A <i>rsbRBΔ2 rsbRCΔ1::ery rsbRDΔ2 amyE::ctc-lacZ trpC2</i>	pTG5948 → PB1078 ^b
PB1103	<i>rsbRA</i> K47A <i>rsbRBΔ2 rsbRCΔ1::ery rsbRDΔ2 amyE::ctc-lacZ trpC2</i>	pTG5949 → PB1078 ^b
PB1104	<i>rsbRA</i> E108A <i>rsbRBΔ2 rsbRCΔ1::ery rsbRDΔ2 amyE::ctc-lacZ trpC2</i>	pTG5950 → PB1078 ^b
PB1106	<i>rsbRA</i> K93A <i>rsbRBΔ2 rsbRCΔ1::ery rsbRDΔ2 amyE::ctc-lacZ trpC2</i>	pTG5975 → PB1078 ^b
PB1109	<i>rsbRAΔ2 rsbRBΔ2 rsbRCΔ1::ery rsbRDΔ2 amyE::ctc-lacZ trpC2</i>	pTG5979 → PB1078 ^b
PB1133	<i>rsbRA</i> L55R V57R <i>rsbRBΔ2 rsbRCΔ1::ery rsbRDΔ2 amyE::ctc-lacZ trpC2</i>	pTG5981 → PB1078 ^b
PB1141	<i>rsbRA</i> E136K <i>rsbRBΔ2 rsbRCΔ1::ery rsbRDΔ2 amyE::ctc-lacZ trpC2</i>	pTG5998 → PB1078 ^b
PB1144	<i>rsbRA</i> K82A K93A <i>rsbRBΔ2 rsbRCΔ1::ery rsbRDΔ2 amyE::ctc-lacZ trpC2</i>	pTG6003 → PB1080 ^b
PB1150	<i>rsbRA</i> K82A <i>rsbS</i> S59A <i>rsbRBΔ2 rsbRCΔ1::ery rsbRDΔ2 amyE::ctc-lacZ trpC2</i>	pTG6009 → PB1080 ^b
PB1159	<i>rsbRA</i> V41R <i>rsbRBΔ2 rsbRCΔ1::ery rsbRDΔ2 amyE::ctc-lacZ trpC2</i>	pTG5999 → PB1078 ^b
PB1161	<i>rsbS</i> S59A <i>rsbRBΔ2 rsbRCΔ1::ery rsbRDΔ2 amyE::ctc-lacZ trpC2</i>	pTG6009 → PB1078 ^b
PB1181	<i>rsbRA</i> K82A <i>amyE::ctc-lacZ trpC2</i>	pTG5926 → PB198 ^b
PB1191	<i>rsbRA</i> E136K <i>amyE::ctc-lacZ trpC2</i>	pTG5998 → PB198 ^b
PB1201	<i>rsbRA</i> E136K <i>rsbS</i> S59A <i>rsbRBΔ2 rsbRCΔ1::ery rsbRDΔ2 amyE::ctc-lacZ trpC2</i>	pTG6009 → PB1141 ^b
PB1209	<i>rsbRA</i> K82A K93A <i>rsbS</i> S59A <i>rsbRBΔ2 rsbRCΔ1::ery rsbRDΔ2 amyE::ctc-lacZ trpC2</i>	pTG6009 → PB1144 ^b
PB1210	<i>rsbRA</i> K82A K93A <i>amyE::ctc-lacZ trpC2</i>	pTG6003 → PB198 ^b
PB1213	<i>rsbRA</i> K93A <i>rsbS</i> S59A <i>rsbRBΔ2 rsbRCΔ1::ery rsbRDΔ2 amyE::ctc-lacZ trpC2</i>	pTG6009 → PB1106 ^b

^a Arrow indicates transformation from donor to recipient.

^b Two-step allele replacement.

^c Linearized plasmid.

using a single-copy transcriptional fusion between the well-characterized *ctc* promoter and a *lacZ* reporter (8).

β-Galactosidase accumulation assays. Shake cultures were grown at 37°C to mid-exponential phase in buffered Luria broth lacking salt (BLB) (7) and then diluted 1:25 into fresh BLB. Culture densities were monitored with a Klett-

TABLE 2. Plasmids used for strain construction

Plasmid	Alteration or relevant feature	Reference or source
pDH32-ctc	<i>ctc-lacZ</i> fusion, for integration at <i>amyE</i>	8
pSS4332	Expresses I-SceI for two-step allele replacement	11
pSA82	pUC19:: <i>rsbRCΔ1::ery</i>	1
pTG5916	pUS19 integrative plasmid; NdeI site converted to I-SceI	This study
pTG5923	<i>rsbRA</i> in pTG5916	This study
pTG5924	<i>rsbRA</i> E60A in pTG5916 (GAA → GCA)	This study
pTG5925	<i>rsbRBΔ2</i> in pTG5916 (codons 19-266 deleted)	This study
pTG5926	<i>rsbRA</i> K82A in pTG5916 (AAG → GCG)	This study
pTG5927	<i>rsbRA</i> E126A in pTG5916 (GAA → GCA)	This study
pTG5943	<i>rsbRDΔ2</i> in pTG5916 (codons 11-265 deleted)	This study
pTG5944	<i>rsbRA</i> T86A in pTG5916 (ACT → GCG)	This study
pTG5945	<i>rsbRA</i> N129A in pTG5916 (AAT → GCG)	This study
pTG5948	<i>rsbRA</i> Y35A in pTG5916 (TAT → GCT)	This study
pTG5949	<i>rsbRA</i> K47A in pTG5916 (AAA → GCA)	This study
pTG5950	<i>rsbRA</i> E108A in pTG5916 (GAG → GCG)	This study
pTG5975	<i>rsbRA</i> K93A in pTG5916 (AAG → GCG)	This study
pTG5979	<i>rsbRAΔ2</i> in pTG5916 (codons 2-145 deleted)	This study
pTG5981	<i>rsbRA</i> L55R V57R in pTG5916 (CTG → CGA, GTT → CGT)	This study
pTG5998	<i>rsbRA</i> E136K in pTG5916 (GAA → AAA)	This study
pTG5999	<i>rsbRA</i> V41R in pTG5916 (GTG → CGA)	This study
pTG6003	<i>rsbRA</i> K82A K93A in pTG5916 (AAG → GCG; AAG → GCG)	This study
pTG6009	<i>rsbS</i> S59A in pTG5916 (TCA → GCA)	This study
pUS19	Integrative plasmid	6

Summerson colorimeter equipped with a number 66 (red) transmission filter. Samples were collected from unstressed cells during exponential growth up to a density of 20 Klett units, when different amounts or kinds of stressors were added to the final concentrations indicated in the figures. All samples were treated essentially according to Miller (27), as previously described (24). Protein concentrations were determined with a Bio-Rad protein assay (Bio-Rad Laboratories, Hercules, CA), and enzyme activity was defined as $\Delta A_{420} \times 1,000 \text{ min}^{-1} \text{ mg}^{-1}$. Assays were done under moderate white light (3 to 4 $\mu\text{mol m}^{-2} \text{ s}^{-1}$) from fluorescent room illumination, which would normally saturate the YtvA blue-light activator of σ^B (4). Light intensity was measured using a Black Comet model CXR-SR spectroradiometer equipped with a CR2 UV-Vis-NIR cosine receptor (Stellar Net Inc., Tampa, FL).

Basal activity was defined as the activity in unstressed cells sampled at 20 Klett units; stress activation was defined as the difference between this basal value and maximum activity after ethanol or salt stress. The PB1078 parent used to assess the effects of RsbRA substitutions (and bearing null *rsbRB*, *rsbRC*, and *rsbRD* alleles) had an 8-fold-higher basal activity than the PB198 wild-type control (with its full complement of four RsbR coantagonists): 84 versus 10 units. However, the PB1078 parent was similar to the PB198 wild type with respect to activation in response to 4% ethanol stress: 1,282 versus 1,224 units. These activities are the averages from at least five experiments.

Detection of RsbRA by Western blotting. Mouse monoclonal anti-RsbRA antibody was kindly provided by William Haldenwang (15). Antibody specificity was verified and Western blots were done as previously described (24). Briefly, cells were grown at 37°C to mid-exponential phase in BLB, harvested by centrifugation, and broken by sonication. Protein samples (40 μg) from wild-type and mutant extracts were separated by SDS-PAGE and transferred to polyvinylidene difluoride membranes (Bio-Rad). Detection of cross-reacting material using primary and secondary antibody and an ECL Plus kit (Amersham Pharmacia Biotech, Piscataway NJ) was carried out as previously described (24).

Selection of candidate interaction sites on the N-terminal domain of RsbRA. In addition to examining residues previously identified by others, we manually inspected the dimer crystal structure (Protein Data Bank [PDB] code 2BNL [28]) for surface features characteristic of protein-protein contacts. Specifically, we

looked for exposed nonpolar surfaces and nearby concentrations of charged side chains. Five separate surfaces were targeted; the asterisk within each category indicates a polar or amphiphilic residue substituted with alanine or a nonpolar residue substituted with arginine. (i) L55* and V57* comprise a solvent-accessible hydrophobic patch along with Y8, A12, L54, and A62; (ii) Y35* is prominently displayed in the so-called CD corner (28), with (iii) a nearby hydrophobic patch composed of L37, V41*, and I77; (iv) on the periphery, far from the dimer groove, K47* forms a salt bridge with D51 and is bounded by nonpolar L19, I50, L54, and L55; and (v) near the dimer interface and on the opposite side from the α -helical linker to the STAS domain, E108* flanks a disordered charged loop and is adjacent to E111. The three-dimensional locations of these residues are displayed in Fig. 2.

RESULTS

Phenotypes of mutants with dimer groove substitutions do not correlate with predictions of previous *in vitro* assays. Based on the structural similarities between the N-terminal, nonheme globin domain of RsbRA and related domains of other proteins, such as KaiA and HemAT, Murray et al. (28) proposed that the prominent groove formed by an N-terminal homodimer (Fig. 2) provides a site of interaction both for hypothetical effector proteins and for the RsbT kinase. Effector binding was suggested to displace RsbT from the stressosome and activate environmental signaling. Consistent with this proposal, Hardwick et al. (19) noted structural similarities between the N-terminal domain of RsbRA and the established site of interaction of RsbT with its alternate binding partner, RsbU. Moreover, any of three substitutions located on the surface of the N-terminal dimer groove (E60A, K82A, and E126A) prevented RsbT binding to the stressosome *in vitro*, whereas two other groove substitutions (T86A and N129A) were indistinguishable from wild-type RsbRA in this regard (28).

We further tested this proposal by determining the *in vivo* phenotypes caused by the same five N-terminal substitutions studied by Murray et al. (28). Our experimental approach considered two salient features of the system. First, *rsbRA* mutations must be evaluated in their normal chromosomal context, in which the *rsbRA-rsbS-rsbT* genes are cotranscribed and translated (31). Second, the negative function of RsbRA is partly redundant with its paralogs RsbRB, -C, and -D (24, 32). Therefore, to reveal the true phenotype caused by each N-terminal substitution, we exchanged the allele of interest with the wild-type, chromosomal copy of *rsbRA* in a strain missing the other three members of the coantagonist family. We then measured the effect of each substitution using a single-copy transcriptional fusion whose expression was fully dependent on σ^B . Contrary to expectations, predictions from the earlier *in vitro* assays were not confirmed by the phenotypes we observed.

Substitutions unable to bind RsbT *in vitro* would be expected to generate high σ^B activity *in vivo*, even in unstressed cells, whereas those that avidly bound RsbT would behave like the parent strain. However, we found only modest phenotypes, and these had little correspondence to the results of the earlier study. For example, the T86A and N129A substitutions, which effectively bound RsbT when formed into stressosomes *in vitro* (28), nonetheless manifested a 2- to 3-fold increase in σ^B activity in unstressed cells (Fig. 3A). This elevated activity was greater than that elicited by the E60A and E126A substitutions, which were unable to bind RsbT *in vitro*. In contrast, the K82A substitution, grouped by Murray et al. (28) with E60A

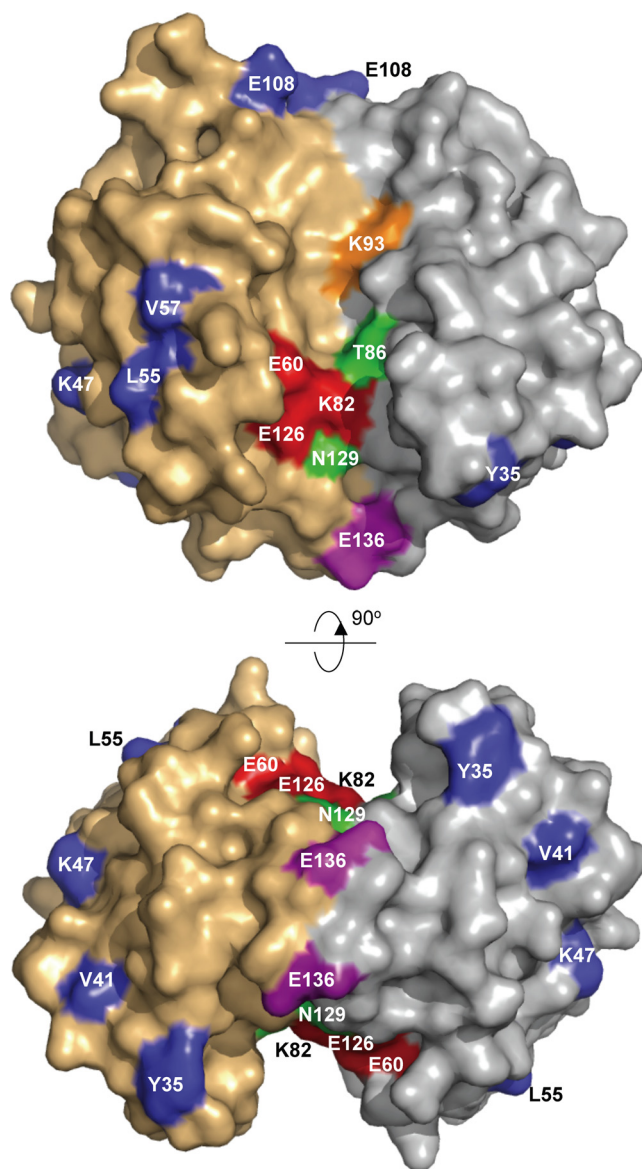


FIG. 2. Locations of altered residues within the homodimer formed by the nonheme globin domain of RsbRA. The three-dimensional structure (PDB code 2BNL) is from Murray et al. (28). The surface of one monomer is shown in gold, the other in silver. (Top) View showing one dimer groove, containing E60, K82, T86, K93, E126, and N129. Residues at which single alanine substitutions prevented RsbT binding in a previous *in vitro* assay (28) are color-coded red, whereas those that did not affect RsbT binding are green; the K93 residue predicted to contribute to dimer formation is orange; the site of the E136K substitution (31) is magenta; other prominent surface residues altered in this study are blue. (Bottom) Ninety-degree view of both dimer grooves, seen from the vantage point of the 13-residue α -helical linkers (not shown) that connect the N-terminal nonheme globin domains and the C-terminal STAS domains. E136 is the last residue of the N-terminal domain.

and E126A, gave the strongest phenotype, with a 4- to 5-fold increase in unstressed cells. We conclude that the phenotype of elevated σ^B activity in unstressed cells was not simply correlated with the previously measured biochemical property of mutant stressosomes to bind RsbT *in vitro*.

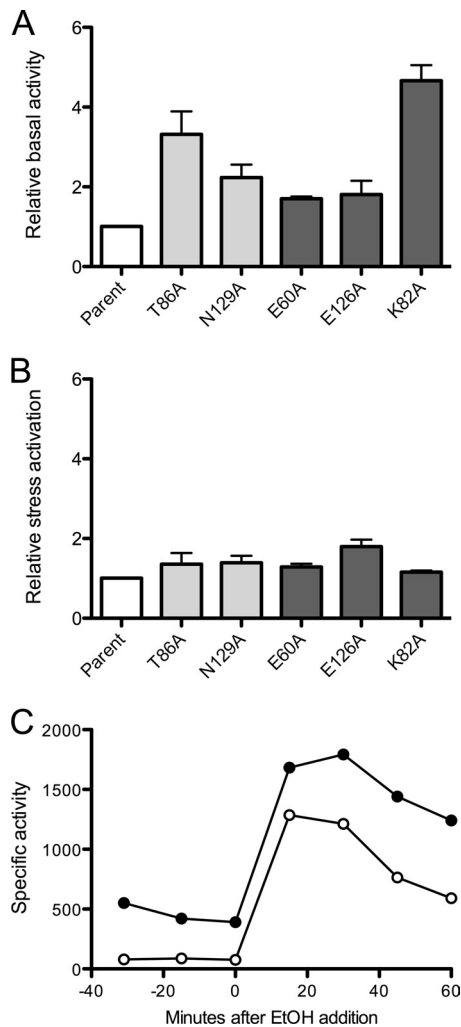


FIG. 3. Effects of dimer groove substitutions on σ^B activity in stressed and unstressed cells. (A) Relative basal activity in unstressed cells, with the white bar showing the parent strain (PB1078, encoding only the RsbRA coantagonist) taken as 1. Light-gray bars indicate congenic strains bearing RsbRA substitutions found to bind RsbT *in vitro* (28), i.e., T86A (PB1092) and N129A (PB1093); dark-gray bars indicate strains bearing substitutions unable to bind RsbT *in vitro*, i.e., E60A (PB1079), E126A (PB1081), and K82A (PB1080). Basal activity (β -galactosidase accumulation from a *ctc-lacZ* fusion) was measured in logarithmically growing cells before stress addition, at a culture density of 20 Klett units; in these experiments, the average basal activity for the PB1078 parent was 104 units. Error bars indicate standard errors of the means (SEM) from at least two independent assays. (B) Relative activation following 4% ethanol stress, with the level for the parent strain taken as 1. Stress activation was the change between basal and maximum activity after ethanol addition; in these experiments, the average activation for the PB1078 parent was 1,196 units. The y axes of panels A and B are the same to facilitate comparison. (C) Results from a representative assay yielding data for panels A and B. Open circles indicate β -galactosidase accumulation in the parent strain (PB1078); closed circles are a strain bearing K82A (PB1080). Basal activity (defined for panel A) is shown here at time zero; maximum activity was either 15 or 30 min after ethanol (EtOH) addition.

We also tested the effects of each of the five alleles on response to 4% ethanol stress. Here also, there was no correlation with the previous *in vitro* assays. Moreover, the mutant alleles generally had a weaker and nonparallel influence on

stress response (Fig. 3B) than they did on basal activity in unstressed cells (Fig. 3A). This was particularly evident for the K82A allele, which had the strongest effect on basal activity but no significant impact on stress response. To better illustrate this result, we show in Fig. 3C results from a typical full assay of the mutant bearing K82A. Here the maximum response to 4% ethanol stress was shifted only by the difference in basal level between the K82A strain and its parent, and the stress-induced increase in σ^B activity was the same in both strains. The results of multiple similar assays are summarized in the bar graphs of Fig. 3A and B, both for the K82A mutant and for the other mutants. We conclude that the ability to respond to 4% ethanol stress *in vivo* is not correlated with the previously measured ability of the mutant stressosomes to bind RsbT *in vitro*.

We should note that, in addition to RsbRA, the strains in these experiments contained another RsbR paralog within their stressosomes—the YtvA blue-light sensor (3, 17). Genetic analysis suggests that YtvA does not function as a coantagonist like RsbRA, -B, -C, and -D and instead has only a positive role in σ^B activation (1, 3, 5, 17). To determine if the presence of YtvA somehow contributed to the discrepancy between our *in vivo* results and the *in vitro* results of Murray et al. (28), we introduced a *ytvA* deletion into the strain background and repeated the *in vivo* assays. As expected, σ^B activity decreased in all strains (data not shown). However, the relative activities in strains bearing the N-terminal substitutions remained the same as those in the assays with results shown in Fig. 3. Because the presence of YtvA improved the sensitivity of the assay without otherwise affecting the relative order of the results, we used strains wild type at the *ytvA* locus for all remaining experiments.

Substitutions predicted to affect dimerization significantly influence signal output in unstressed cells. The five substitutions examined thus far all lie near one another on the surface of the dimer groove (Fig. 2). Inspection of the available crystal structure suggested that these residues also form an intradimer hydrogen-bonded network. K82 is central to this network and makes extensive intersubunit hydrogen-bonded contacts with E60, E126, and either T125 or P122. K82 positioning may be further stabilized by intra- and intersubunit hydrogen bonds with T86 and N129, respectively. The intricacy of this network suggests that the K82A substitution would significantly affect dimer stability or structure.

We therefore wished to explore the effect of another substitution predicted to affect dimer strength but not associated with the K82 network. K93 lies on the surface of the dimer groove and makes a buried, intersubunit salt link with D117; it is separated from K82 by 17 Å and lies in a different molecular context (Fig. 2). When assayed in unstressed cells of a strain encoding only the RsbRA coantagonist, the K93A substitution increased σ^B activity more than 4-fold relative to the parent—about the same as the K82A substitution (Fig. 4A). Moreover, the effect of combining K93A with K82A was essentially multiplicative, with a 15-fold increase over the parent activity.

For comparison, we also examined a strain bearing the E136K substitution, identified by Reeves and Haldenwang (31) during a random screen for dominant mutations that affect stressosome function. Prior to our study, the E136K mutant was the only N-terminal substitution mutant whose phenotype

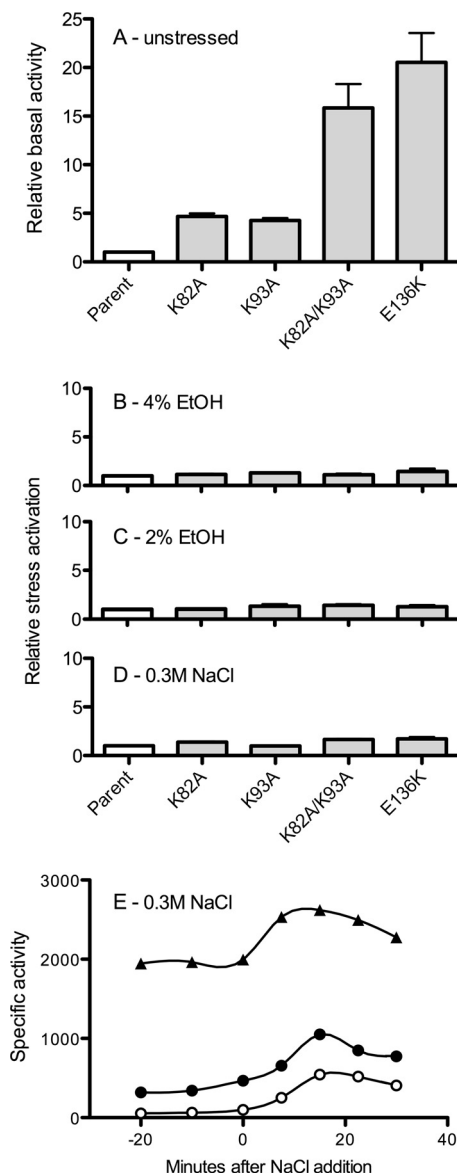


FIG. 4. Other substitutions with significant effect on basal activity had little impact on stress response. (A) Relative basal activity in unstressed cells, with the white bar showing the parent strain (PB1078, encoding only the RsbRA coantagonist) taken as 1. Light-gray bars indicate congenic strains bearing RsbRA substitutions K82A (PB1080), K93A (PB1106), K82A K93A (PB1144), and E136K (PB1141). Basal activity was measured as described in the legend for Fig. 3A; in these experiments, the average basal activity for the PB1078 parent was 90 units. Error bars indicate SEM from at least two independent assays. (B to D) Relative activation following 4% ethanol stress, 2% ethanol stress, or 0.3 M NaCl stress, with the level for the parent strain taken as 1. Stress activation was measured as defined in the legend for Fig. 3B; in these experiments, the average activation for the PB1078 parent was 1,360 units (B), 1,101 units (C), or 444 units (D). The y axes of panels A to D have the same scale to facilitate comparison. (E) Results from a representative assay yielding data for panels A to D. Open circles indicate β -galactosidase accumulation in the parent strain (PB1078), closed circles are a strain bearing K82A (PB1080), and closed triangles are a strain bearing E136K (PB1141).

had been examined *in vivo*, and this substitution was found to affect σ^B activity primarily in unstressed cells. However, these earlier assays were done in a strain encoding all RsbR paralogs, and the authors pointed out that any impact on stress signaling could be masked by the redundant function of other family members.

We therefore assayed the E136K phenotype in a strain in which RsbRA was the only functional coantagonist and found that it increased σ^B activity 20-fold in unstressed cells (Fig. 4A). This is similar to the effect that Reeves and Haldenwang observed in a strain with all four coantagonists. E136 is the last residue of the N-terminal, nonheme globin domain (28), and it lies adjacent to the 13-residue α -helical linker that connects the N- and C-terminal domains (26). Given its position in the crystal structure, E136K is not expected to affect dimerization of the N-terminal domain, and the proximal basis of its dysfunction likely differs from that for K82A or K93A (Fig. 2). Nonetheless, strains bearing either E136K or the K82A K93A double mutation manifested similarly high σ^B activities in unstressed cells (Fig. 4A). These high basal activities represent about one-third of the activity of the fully deregulated system, defined as the activity observed in strains missing all four RsbR coantagonists or the RsbS antagonist (data not shown).

Notably, even the E136K and K82A K93A substitutions, with their strong impact on basal activity, had less than a 2-fold effect on response to stresses of different strengths and kinds (Fig. 4B to D). These results extend the generality of the phenotypes observed in experiments with results shown in Fig. 3: maximum stress response was shifted only by the difference in basal level between the mutant and its parent, and the stress-induced increases in σ^B activity were similar in all strains. This phenomenon is underscored in the representative salt stress assay with results shown in Fig. 4E. Here the basal levels of the three strains differ strikingly, with even the maximum responses of the parent and K82A mutant remaining well below the basal level of the E136K mutant, and yet all three have comparable stress responses. Because the tested N-terminal substitutions manifested similar amplitudes of fusion expression following stress, we conclude that none significantly affected the sensitivity of stress detection.

Suppression analysis indicates that the K82A or the E136K protein can form functional stressosomes. The results in Fig. 3 and 4 show that the tested substitutions had a differential effect on the two states examined: basal output of the system in unstressed cells increased, whereas amplitude of the stress response remained largely unaffected. The RsbRA regulator is known to have both positive and negative roles (2). The positive function is thought to reflect the ability of RsbRA to enhance the phosphorylation of RsbS by RsbT during the stress response, which is associated with RsbT release (10, 18, 25). In contrast, the negative function reflects the requirement for RsbRA to act as a coantagonist with RsbS to sequester RsbT within the stressosome; RsbS alone is unable to effectively bind RsbT *in vitro* or prevent constitutively high signaling *in vivo* (9, 24). The N-terminal substitutions could conceivably affect either the positive or the negative function of RsbRA. For example, they could alter the positive function by increasing the phosphorylation of RsbS, leading to greater RsbT release in unstressed cells. On the other hand, they could alter the negative function if the mutant RsbRA proteins were pres-

ent at less than wild-type levels or were less capable of forming stressosomes *in vivo*; these defects might impact the ability of the stressosome to bind RsbT and keep basal output low. We performed a genetic suppression experiment to distinguish these possibilities.

Alteration of the conserved serine in RsbS to alanine (S59A) prevents phosphorylation by RsbT (35). We combined the RsbS S59A substitution with each of the four strongest *rsbRA* mutations in a background in which RsbRA was the only coantagonist present and found that the basal output of K82A- and E136K-bearing strains returned to the low level of the parent (Fig. 5A). Notably, RsbS S59A did not significantly diminish the ability of these strains to respond to 4% ethanol stress (Fig. 5B). A similar lack of RsbS S59A influence on stress response was reported in a strain engineered to express another single RsbR paralog, RsbRC (24). Thus, the suppression of the basal phenotypes noted in Fig. 5A was not due to a general signaling defect introduced by the RsbS substitution.

Because RsbS S59A completely suppressed the K82A and E136K phenotypes, we infer that these substitutions increase basal output by increasing the phosphorylation level of RsbS S59 in unstressed cells. Although we cannot eliminate the possibility that RsbS S59A acts as a bypass suppressor, counteracting the effects of K82A and E136K by a means unrelated to their primary defects, its ability to fully suppress two such quantitatively different phenotypes argues that RsbS S59 lies on the signaling pathway directly affected by K82A or E136K. More importantly, because neither wild-type RsbS nor its S59A form can by itself reverse the high level of σ^B activation caused by loss of RsbR coantagonist function (1, 24, 32), this correction of the basal phenotype indicates that the stressosome complement in the suppressed strains was fully capable of binding RsbT and holding the system in a nonsignaling state. We draw the strong inference that K82A and E136K do not adversely affect RsbRA levels or the ability to form functional stressosomes. This inference is in accord with the earlier immunological and biochemical analysis of Reeves and Haldenwang (31), who found that E136K had no observable effect on these properties.

In contrast, the K93A phenotype was not suppressed by the presence of RsbS S59A, and the K82A K93A phenotype was only partly suppressed (Fig. 5A). This partial suppression was consistent with the ability of S59A to correct the K82A but not the K93A defect. These results suggest that K93A acts by a different mechanism than K82A or E136K. However, they provide no information regarding the ability of strains bearing the K93A or K82A K93A substitutions to form functional stressosomes.

In the absence of a positive suppression result for K93A or K82A K93A, we next asked if these substitutions affected RsbRA synthesis or stability. Estimating RsbRA levels by probing cell extracts with a monoclonal anti-RsbRA antibody, we found that strains encoding K93A or E136K manifested about the same RsbRA signal as the parent strain (Fig. 5C). However, strains encoding K82A or K82A K93A had no detectable signal. This result was unexpected because the K82A phenotype was fully corrected by the RsbS S59A suppressor and K82A K93A was partly corrected (Fig. 5A). The suppression results indicate that RsbRA was present in these strains at levels sufficient to form stressosomes capable of bind-

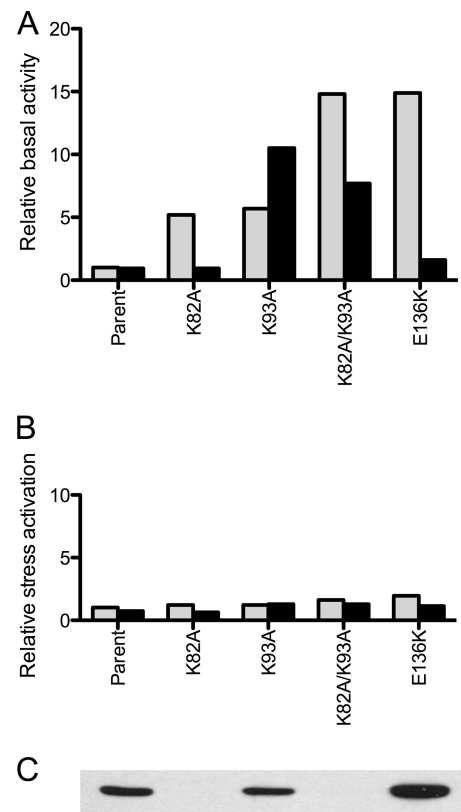


FIG. 5. Genetic suppression analysis indicates that RsbRA proteins with K82A or E136K substitutions form functional stressosomes. (A) Relative basal activities elicited by the indicated RsbRA substitution are shown by light-gray bars; activities conferred by the same substitution coupled with the S59A substitution of RsbS are shown by black bars. All are expressed relative to the activity of the parent (PB1078, encoding only the RsbRA coantagonist), taken as 1. Basal activity was measured as described in the legend for Fig. 3A; in these experiments, the average basal activity for the PB1078 parent was 88 units. Other congenic strains include the parent with the S59A substitution (PB1161), the K82A mutant without (PB1080) and with (PB1150) S59A, the K93A mutant without (PB1106) and with (PB1213) S59A; the K82A K93A mutant without (PB1144) and with (PB1209) S59A, and the E136K mutant without (PB1141) and with (PB1201) S59A. (B) Relative activation following 4% ethanol stress, with the level for the parent strain taken as 1. Stress activation was measured as defined in the legend for Fig. 3B; in these experiments, the average activation for the PB1078 parent was 1,372 units. Strains and bar representations are defined above. (C) Relative levels of wild-type and mutant RsbRA proteins estimated by Western blotting. Extracts from each strain bearing the RsbRA substitution shown in the column above the blot were separated by PAGE and probed with monoclonal anti-RsbRA antibody. The K82A substitution apparently removed the epitope required for antibody interaction.

ing RsbT. The simplest explanation for the negative Western result is that K82A removes the epitope recognized by the monoclonal antibody.

Other surface substitutions have little effect on system properties. We wished to explore the notion that other surfaces of the N-terminal domain might be important for environmental signaling, perhaps by providing sites of interaction with other cellular components. The N-terminal domains of all four RsbR coantagonists found in *B. subtilis* are predicted to be structurally similar, but they share low sequence similarity (28). In the

TABLE 3. Effect of N-terminal surface alterations on σ^B activity^a

Strain	RsbRA substitution(s)	Location	Basal level ^b (SEM)	Stress activation ^c (SEM)
PB1078	None (parent)	Control	1.0	1.0
PB1102	Y35A	CD corner	1.3 (0.10)	1.1 (0.01)
PB1103	K47A	Charged patch	0.9 (0.08)	1.0 (0.26)
PB1104	E108A	Charged patch	0.9 (0.03)	0.9 (0.15)
PB1133	L55R V57R	Hydrophobic patch	1.4 (0.14)	1.1 (0.28)
PB1159	V41R	Hydrophobic patch	1.0 (0.28)	1.3 (0.52)

^a Activity measured using a *ctc-lacZ* transcriptional fusion in two independent experiments.

^b Basal level in unstressed cells, relative to that for the PB1078 parent.

^c Stress activation is the difference between the basal level in unstressed cells and the maximum level following 4% ethanol stress, relative to activation in the parent.

absence of any clues provided by sequence conservation, we manually inspected the crystal structure of the RsbRA N-terminal domain and chose five features for further investigation (see Materials and Methods). These included a tyrosine residue that forms a prominent part of the CD corner, suggested by others (28) as a region of interest, and also residues whose modification was designed to disrupt either a charged cluster or a hydrophobic patch (Fig. 2). When assayed in a strain missing RsbRB, -C, and -D, none of these RsbRA substitutions by themselves had a significant effect on either basal output or stress response (Table 3).

We also attempted to determine the overriding function of the N-terminal domain by means of a large, in-frame deletion that removed the region coding for the nonheme globin and the adjacent 13-residue linker (residues 3 to 145). The remaining STAS domain of RsbRA (residues 146 to 274) is able to assemble into a stressosome when complexed with RsbS *in vitro* (26). However, we were unable to establish whether this STAS domain could assemble into a stressosome *in vivo*. We replaced wild-type *rsbRA* with the allele encoding only the STAS domain in the genetic background in which the other three coantagonists were absent and found that the resulting strain manifested extremely high reporter activity (data not shown). This activity could not be corrected by the RsbS S59A suppressor, nor could we detect any RsbRA signal in Western blots of cell extracts, which was not unanticipated if the deleted K82 in fact represents an epitope required for recognition. Absent any evidence that the mutant protein is present at normal levels or can form a functional stressosome, we cannot address the direct effect the N-terminal deletion might have on signaling.

Mutant phenotypes are masked in the presence of other RsbR paralogs. Our experimental approach—use of a strain expressing only RsbRA—was designed to uncover the effect of each substitution without interference from the other RsbR coantagonists. For comparison, we also determined the phenotypes caused by selected substitutions in a strain that was otherwise wild type, encoding all of the RsbR paralogs. Notably, the phenotype caused by the K82A substitution, which was the strongest of the five originally studied by Murray et al. (28), was completely masked by the presence of RsbRB, -C, and -D in the wild-type background (Fig. 6). In contrast, the pheno-

type caused by the E136K substitution was much the same in both backgrounds. This was not surprising, considering that E136K was originally identified and characterized in a wild-type strain (31). To distinguish whether this difference in response in the wild type reflected a qualitative or quantitative effect of the altered residue, we also examined the K82A K93A double substitution. This is akin to K82A in terms of its potential effect on dimerization and groove formation and akin to E136K in terms of the magnitude of its effect on σ^B activity in unstressed cells. In the wild-type background, the K82A K93A phenotype was also completely masked by the presence of RsbRB, -C, and -D (Fig. 6). Thus, of the substitutions we examined, only the E136K phenotype was apparent in otherwise wild-type cells.

DISCUSSION

Genetic, biochemical, and structural analyses indicate that a minimal stressosome comprises RsbRA, RsbS, and RsbT (9, 23, 24, 26). Moreover, a bioinformatics analysis found homologs of RsbRA, RsbS, and RsbT encoded by contiguous genes in a wide array of bacteria, suggesting that these three proteins form a sensory and transmission module that can be coupled to different signaling networks (29). However, only in *B. subtilis* and *Listeria monocytogenes* is the physiological role of the module known, i.e., activation of the σ^B general stress factor in response to environmental signals (30, 34). We investigated the mechanism of signal transmission in the *Bacillus* model by making substitutions within the N-terminal, nonheme globin domain of RsbRA, the presumed sensing domain of the module (26). Our study has three findings.

First, even the strongest phenotypes elicited by our *rsbRA* mutations were masked by the presence of the other RsbR coantagonists (Fig. 6). An exception was the E136K phenotype, identified earlier by Reeves and Haldenwang (31). On the other hand, these authors had indicated uncertainty regarding the effect of E136K on stress activation when assayed in a strain bearing the full complement of RsbR paralogs. Thus,

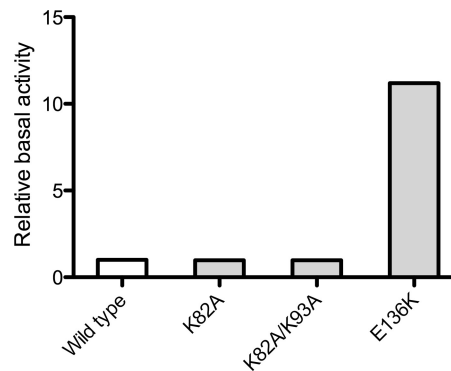


FIG. 6. The wild-type background masks the phenotypes caused by two representative N-terminal substitutions. Relative basal activity in unstressed cells, with the white bar showing the level for the wild-type strain (PB198, encoding all four members of the RsbR coantagonist family) taken as 1; the average basal activity of this control was 10 units. Light-gray bars show activities of congenic strains bearing RsbRA substitutions K82A (PB1181), K82A K93A (PB1210), and E136K (PB1191).

our experimental approach—using a strain expressing only RsbRA—was key to revealing the phenotype caused by each substitution.

Second, the phenotypes elicited by substitutions within the N-terminal dimer groove of RsbRA did not agree with predictions resulting from biochemical analysis of the same mutant proteins assembled into stressosomes *in vitro*. As shown in Fig. 3, the *in vivo* assay was required to capture the effect of each substitution on stressosome output. We conclude that the basic ability of wild-type and mutant stressosomes to bind RsbT *in vitro*, which figured prominently in earlier studies (10, 28), has limited predictive power *in vivo*. These earlier studies used size exclusion chromatography to qualitatively assess RsbT binding to a stressosome core consisting of RsbRA and RsbS. However, such assays could not control other factors that may affect stressosome function, such as the *in vivo* concentrations of its constituent proteins, their cellular environment, or their *in vivo* level of phosphorylation.

In contrast, we assayed the effects of each N-terminal substitution on system output, which takes into account its influence on all elements in the signaling pathway. In this regard, the suppression results shown in Fig. 5 indicate that the elevated basal output elicited by the K82A substitution in RsbRA can be completely corrected by the S59A substitution in RsbS. This result calls into question the earlier interpretation that the K82A substitution significantly interferes with RsbT binding to the N-terminal domain of RsbRA (28) and implies that it acts instead by increasing the phosphorylation levels of RsbS. Consistent with this revised interpretation, Murray et al. (28) were unable to detect interaction between RsbT and the N-terminal domain, suggesting that determinants external to the domain contributed more to the strength of RsbT binding to the stressosome. Moreover, structural studies of a static stressosome showed RsbT positioned over RsbS, not RsbRA (26). Thus, other than the *in vitro* assay, the interpretation of which is now open to question, there are presently no experimental data to support the model in which the N-terminal domain of RsbRA provides important contacts for RsbT binding, which is then displaced by competing effector proteins (28).

Third, substitutions within the N-terminal region that manifested a significant phenotype elevated basal output of the system only in unstressed cells and had little impact on subsequent stress signaling (Fig. 3 and 4). Thus, the stressosome functions we examined—basal output and stress signaling—appear to be genetically separable. One explanation is that a distinct stress-signaling pathway was indeed untouched by our substitutions. In this view, the true stress-signaling pathway remains to be discovered and may not in fact initiate within the N-terminal domain. However, another possibility is that the stressosome itself has considerable signaling capacity and that our substitutions impacted only a fraction of that reserve. Distinguishing these alternatives may involve isolating *rsbRA* mutants that are unable to signal. The locations within the RsbRA protein of the alterations they encode would also address the question of which regions are involved in signal sensing and which are involved in signal transmission.

Despite this uncertainty, the present analysis indicates that (i) substitutions within the N-terminal domain of the RsbRA coantagonist can influence stressosome function, as reflected by their significant impact on basal output, and (ii) the effects

of these substitutions are likely communicated to the RsbS antagonist, as reflected by the ability of the S59A alteration within RsbS to suppress a subset of them. However, the results thus far provide no support for the hypothesis that the N-terminal domain functions as a stress sensor.

ACKNOWLEDGMENTS

We thank William Haldenwang for providing anti-RsbRA antibody, Scott Stibitz for pSS4332, and William Burkholder for pUS19. We also thank Anu Thinda for her assistance in the site-directed mutagenesis and Valley Stewart for his helpful discussions.

This research was supported by Public Health Service grant GM42077 from the National Institute of General Medical Sciences.

REFERENCES

1. Akbar, S., et al. 2001. New family of regulators in the environmental signaling pathway which activates the general stress transcription factor σ^B of *Bacillus subtilis*. *J. Bacteriol.* **183**:1329–1338.
2. Akbar, S., C. M. Kang, T. A. Gaidenko, and C. W. Price. 1997. Modulator protein RsbR regulates environmental signalling in the general stress pathway of *Bacillus subtilis*. *Mol. Microbiol.* **24**:567–578.
3. Ávila-Pérez, M., K. J. Hellingwerf, and R. Kort. 2006. Blue light activates the σ^B -dependent stress response of *Bacillus subtilis* via YtvA. *J. Bacteriol.* **188**:6411–6414.
4. Ávila-Pérez, M., J. B. van der Steen, R. Kort, and K. J. Hellingwerf. 2010. Red light activates the σ^B -mediated general stress response of *Bacillus subtilis* via the energy branch of the upstream signaling cascade. *J. Bacteriol.* **192**:755–762.
5. Ávila-Pérez, M., et al. 2009. In vivo mutational analysis of YtvA from *Bacillus subtilis*: mechanism of light activation of the general stress response. *J. Biol. Chem.* **284**:24958–24964.
6. Benson, A. K., and W. G. Haldenwang. 1993. Regulation of σ^B levels and activity in *Bacillus subtilis*. *J. Bacteriol.* **175**:2347–2356.
7. Boylan, S. A., A. R. Redfield, M. S. Brody, and C. W. Price. 1993. Stress-induced activation of the σ^B transcription factor of *Bacillus subtilis*. *J. Bacteriol.* **175**:7931–7937.
8. Boylan, S. A., A. Rutherford, S. M. Thomas, and C. W. Price. 1992. Activation of *Bacillus subtilis* transcription factor σ^B by a regulatory pathway responsive to stationary-phase signals. *J. Bacteriol.* **174**:3695–3706.
9. Chen, C. C., R. J. Lewis, R. Harris, M. D. Yudkin, and O. Delumeau. 2003. A supramolecular complex in the environmental stress signalling pathway of *Bacillus subtilis*. *Mol. Microbiol.* **49**:1657–1669.
10. Chen, C. C., M. D. Yudkin, and O. Delumeau. 2004. Phosphorylation and RsbX-dependent dephosphorylation of RsbR in the RsbR-RsbS complex of *Bacillus subtilis*. *J. Bacteriol.* **186**:6830–6836.
11. Cybulski, R. J., Jr., et al. 2009. Four superoxide dismutases contribute to *Bacillus anthracis* virulence and provide spores with redundant protection from oxidative stress. *Infect. Immun.* **77**:274–285.
12. de Been, M., C. Francke, R. J. Siezen, and T. Abee. 2011. Novel σ^B regulation modules of Gram-positive bacteria involve the use of complex hybrid histidine kinases. *Microbiology* **157**:3–12.
13. Delumeau, O., C. C. Chen, J. W. Murray, M. D. Yudkin, and R. J. Lewis. 2006. High-molecular-weight complexes of RsbR and paralogs in the environmental signaling pathway of *Bacillus subtilis*. *J. Bacteriol.* **188**:7885–7892.
14. Dubnau, D., and R. Davidoff-Abelson. 1971. Fate of transforming DNA following uptake by competent *Bacillus subtilis*. I. Formation and properties of the donor-recipient complex. *J. Mol. Biol.* **56**:209–221.
15. Dufour, A., U. Voelker, A. Voelker, and W. G. Haldenwang. 1996. Relative levels and fractionation properties of *Bacillus subtilis* σ^B and its regulators during balanced growth and stress. *J. Bacteriol.* **178**:3701–3709.
16. Eymann, C., et al. 2011. In vivo phosphorylation patterns of key stressosome proteins define a second feedback loop that limits activation of *Bacillus subtilis* σ^B . *Mol. Microbiol.* **80**:798–810.
17. Gaidenko, T. A., T. J. Kim, A. L. Weigel, M. S. Brody, and C. W. Price. 2006. The blue-light receptor YtvA acts in the environmental stress signaling pathway of *Bacillus subtilis*. *J. Bacteriol.* **188**:6387–6395.
18. Gaidenko, T. A., X. Yang, Y. M. Lee, and C. W. Price. 1999. Threonine phosphorylation of modulator protein RsbR governs its ability to regulate a serine kinase in the environmental stress signaling pathway of *Bacillus subtilis*. *J. Mol. Biol.* **288**:29–39.
19. Hardwick, S. W., et al. 2007. Structural and functional characterization of partner switching regulating the environmental stress response in *Bacillus subtilis*. *J. Biol. Chem.* **282**:11562–11572.
20. Hecker, M., J. Pané-Farré, and U. Völker. 2007. SigB-dependent general stress response in *Bacillus subtilis* and related gram-positive bacteria. *Annu. Rev. Microbiol.* **61**:215–236.
21. Ho, S. N., H. D. Hunt, R. M. Horton, J. K. Pullen, and L. R. Pease. 1989.

- Site-directed mutagenesis by overlap extension using the polymerase chain reaction. *Gene* **77**:51–59.
22. **Janes, B. K., and S. Stibitz.** 2006. Routine markerless gene replacement in *Bacillus anthracis*. *Infect. Immun.* **74**:1949–1953.
 23. **Kang, C. M., M. S. Brody, S. Akbar, X. Yang, and C. W. Price.** 1996. Homologous pairs of regulatory proteins control activity of *Bacillus subtilis* transcription factor σ^B in response to environmental stress. *J. Bacteriol.* **178**:3846–3853.
 24. **Kim, T. J., T. A. Gaidenko, and C. W. Price.** 2004. A multicomponent protein complex mediates environmental stress signaling in *Bacillus subtilis*. *J. Mol. Biol.* **341**:135–150.
 25. **Kim, T. J., T. A. Gaidenko, and C. W. Price.** 2004. In vivo phosphorylation of partner switching regulators correlates with stress transmission in the environmental signaling pathway of *Bacillus subtilis*. *J. Bacteriol.* **186**:6124–6132.
 26. **Marles-Wright, J., et al.** 2008. Molecular architecture of the “stressosome,” a signal integration and transduction hub. *Science* **322**:92–96.
 27. **Miller, J. H.** 1972. Experiments in molecular genetics. Cold Spring Harbor Laboratory, Cold Spring Harbor, NY.
 28. **Murray, J. W., O. Delumeau, and R. J. Lewis.** 2005. Structure of a nonheme globin in environmental stress signaling. *Proc. Natl. Acad. Sci. U. S. A.* **102**:17320–17325.
 29. **Pané-Farré, J., R. J. Lewis, and J. Stülke.** 2005. The RsbRST stress module in bacteria: a signalling system that may interact with different output modules. *J. Mol. Microbiol. Biotechnol.* **9**:65–76.
 30. **Price, C. W.** 2010. General stress response in *Bacillus subtilis* and related Gram-positive bacteria, p. 301–318. *In* G. Storz and R. Hengge (ed.), *Bacterial stress responses*, 2nd ed. ASM Press, Washington, DC.
 31. **Reeves, A., and W. G. Haldenwang.** 2007. Isolation and characterization of dominant mutations in the *Bacillus subtilis* stressosome components RsbR and RsbS. *J. Bacteriol.* **189**:1531–1541.
 32. **Reeves, A., L. Martinez, and W. Haldenwang.** 2010. Expression of, and in vivo stressosome formation by, single members of the RsbR protein family in *Bacillus subtilis*. *Microbiology* **156**:990–998.
 33. **Sambrook, J., E. F. Fritsch, and T. Maniatis.** 1989. *Molecular cloning: a laboratory manual*, 2nd ed. Cold Spring Harbor Laboratory, Cold Spring Harbor, NY.
 34. **Shin, J. H., M. S. Brody, and C. W. Price.** 2010. Physical and antibiotic stresses require activation of the RsbU phosphatase to induce the general stress response in *Listeria monocytogenes*. *Microbiology* **156**:2660–2669.
 35. **Yang, X., C. M. Kang, M. S. Brody, and C. W. Price.** 1996. Opposing pairs of serine protein kinases and phosphatases transmit signals of environmental stress to activate a bacterial transcription factor. *Genes Dev.* **10**:2265–2275.